Equilibrium Potential for the Postsynaptic Response in the Squid Giant Synapse

R. LLINÁS, R. W. JOYNER, and C. NICHOLSON

From the Marine Biological Laboratory, Woods Hole, Mass. 02543, the Department of Physiology and Biophysics, University of Iowa, Iowa City, Iowa 52242, and the Department of Physiology and Pharmacology, Duke University, Durham, N. C. 27706

ABSTRACT The reversal potential for the EPSP in the squid giant synapse has been studied by means of an intracellular, double oil gap technique. This method allows the electrical isolation of a portion of the axon from the rest of the fiber and generates a quasi-isopotential segment. In order to make the input resistance of this nerve segment as constant as possible, the electroresponsive properties of the nerve membrane were blocked by intracellular injection of tetraethylammonium (TEA) and local extracellular application of tetrodotoxin (TTX). Thus, EPSP's could be evoked in the isolated segment with a minimal amount of electroresponsive properties. The reversal potential for the EPSP (E_{EPSP}) was measured by recording the synaptic potential or the synaptic current during voltage clamping. The results indicate that E_{EPSP} may vary from +15 to +25 mV, which is more positive than would be expected for a 1:1 conductance change for Na^+ and K^+ (approximately −15 mV) and too negative for a pure Na^+ conductance (+40 mV). This latter value (E_{Na}) was directly determined in the voltage clamp experiments. The results suggest that the synaptic potential is probably produced by a permeability change to Na^+ to K^+ in a 4:1 ratio. No change in time-course was observed in the synaptic current at clamp levels of −100 and +90 mV. The implications of a variable ratio for Na^+-K^+ permeability in subsynaptic-postsynaptic membranes are discussed.

INTRODUCTION

The equilibrium potential for the excitatory synaptic potential (E_{EPSP}) in the squid giant synapse has been a subject of recent controversy. Thus, Takeuchi and Takeuchi (1962), and Miledi (1969) have indicated that the E_{EPSP} in in this synapse is similar to that encountered in the neuromuscular junction; that is, the EPSP is supposedly generated by a Na^+ and K^+ conductance change, the ratio of these two conductances being close to unity. On the other hand, Gage and Moore (1969) have suggested that the E_{EPSP} is sufficiently close to E_{Na} for it to be generated by a Na^+ permeability change exclusively.

This controversy has stemmed from difficulties in the measurement of reversal potentials (Werman, 1972), especially when the synaptic junction is distributed over a considerable fraction of a length constant, as is the case in the stellate ganglion. The importance of the distributed nature of this synapse in determining the large variability in reversal potentials (both extrapolated and directly measured) was emphasized by Manalis (1971). He demonstrated that the reversal potential for this EPSP may vary from +50 to −20mV in the same synapse, depending on interelectrode distance and on the anisopotentiality in the postsynaptic fiber. The problem has been further complicated by irregularities in the geometry of the postsynaptic element (Young, 1973), the initial portion of the giant axon. A major requirement, therefore, was to attain a situation as close to isopotential as possible over a length of the postsynaptic fiber.

Using a double intracellular oil injection method, a portion of the postsynaptic element was isolated from the rest of the postsynaptic fiber. Current and voltage clamp experiments on this isolated compartment indicate that the E_{EPSP} is close to E_{Na} but that other ions, probably K^+, may contribute to the EPSP since the E_{EPSP} is 20–25 mV more negative (+18–25 mV) than the E_{Na} (+40–45 mV). A preliminary note on this research has been published (Llinás and Nicholson, 1972).

METHODS

Experiments were performed at the Marine Biological Laboratory, Woods Hole, Mass., and at the Duke Marine Laboratory in Beauford, N.C., using the squid *Loligo pealei*. The giant synapse in the stellate ganglion was isolated from the mantle and placed in oxygenated artificial seawater (Takeuchi and Takeuchi, 1962; Miledi and Slater, 1966; Bloedel et al., 1966). The temperature of the bath was kept constant at 15°C by a Peltier effect system, or otherwise allowed to reach room temperature (17–18°). The fin nerve bundle and the connective tissue which overlay the synapse were then removed after which the actual site of synaptic contact between the pre- and postsynaptic fibers could be visualized. The presynaptic fiber was stimulated with a bipolar extracellular electrode in contact with the fiber, or directly through an intracellular microelectrode located near or at the presynaptic terminal itself.

Double Intracellular Oil Gap

Mineral oil was tinted with Sudan black and pressure injected into the postsynaptic fiber as shown in Fig. 1. The injection was made at the proximal and distal ends of the synaptic junction so that current injected into this isolated pocket could not flow longitudinally toward the cells of origin (proximally), or into the length of the axon (distally). Two techniques were used to inject oil in the gelatinous axoplasm.

(*a*) The site of injection was gently compressed with Teflon-covered tweezers in order to obtain a "roller" type of effect (Baker et al., 1962). At the point of axonal

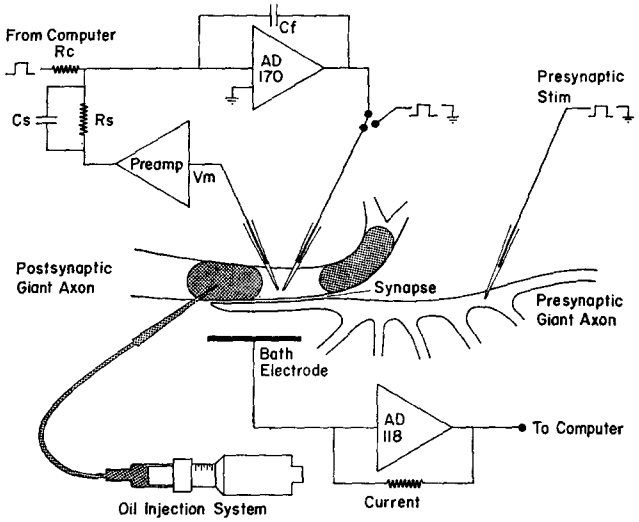

FIGURE 1. Diagram of experimental technique. The oil drop was injected by pressure from a micrometer syringe (shown to the left). The membrane potential level was regulated by a control amplifier (AD 170 ± 100 V) via a feedback loop arrangement. The c ontrol amplifier was fed the membrane potential level through the preamplifier (Preamp) by an R.C. circuit (Rs-Cs). Control pulses were introduced from a PDP-8E computer through the resistance (Rc). The current was injected into the postsynaptic fiber through a second microelectrode and was measured by the AD 118 amplifier (50-kΩ feedback resistance). The presynaptic terminal was activated by means of an intracellular electrode or with an external bipolar electrode.

dimple, oil was injected from the center of the axon so that the oil would spread first spherically and then cylindrically as it entered into contact with the internal surface of the plasma membrane.

(*b*) A second technique consisted of preceding the oil injection with a small Ca^{++} injection (10 mM $CaCl_2$ solution) in order to transform a restricted region of the axoplasmic gel into a sol and thus allow the oil to flow into the axon. This injection was followed by an oil injection from the same pipette, in a manner similar to that described above. The actual effectiveness of the seal was tested directly (see below). About one-fourth of the synapses utilized survived the double oil injection.

Measurement of Efficacy of Intracellular Oil Gap

The efficacy of the oil gap was measured experimentally by means of three intracellular electrodes spaced 750 μm apart in the postaxon adjacent to the synaptic region. The first electrode injected current while the third electrode monitored the resulting potential. The middle electrode was used to inject oil and the changes in the recorded potential during two such oil injections are shown in Fig. 2 A. As the oil drop formed between the current injecting and potential recording electrodes, the potential decreased from a mean value of 39.3 mV to a final mean potential of 9.4 mV, for a 5-μA current.

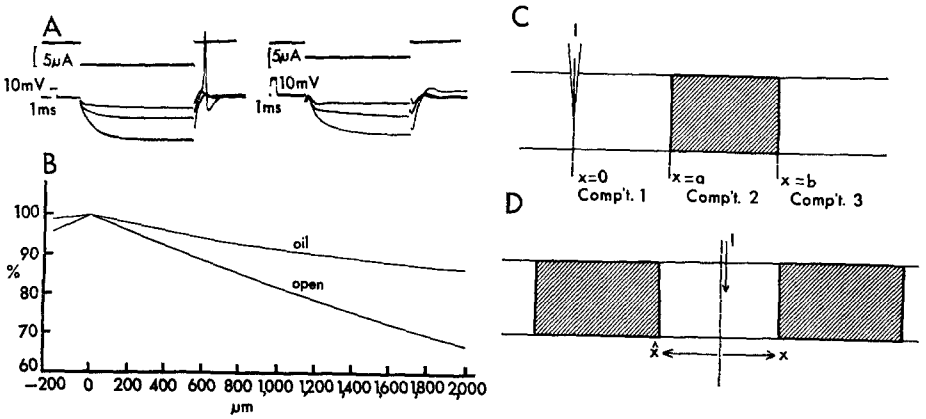

FIGURE 2. Potentials generated in the squid giant axon across an intracellular oil drop. (A) Two examples are illustrated and show three distinct levels of membrane potential produced by the same current pulse as oil is injected between stimulating and recording electrodes. (B) Theoretical comparison of potential decrement with one or two oil drops. A micropipette injects 2.5 μA of current at origin (abscissa) into a 150-μm radius axon. Oil drops, 500 μm long, close the axon at -200 and 2,000 μm. The graph shows the percentage attenuation (ordinate) of the potential with distance from the injection site. For an open axon the attenuation with distance is greater. See text for further details. (C) Geometry for single oil drop calculation. A current I is injected from a micropipette at $x = a$ in the open compartment (1). The oil drop is located between $x = a$ and $x = b$ (compartment 2). The remainder of the axon to the right is open (compartment 3). (D) Geometry for two oil drop calculation. Current flows into compartment formed between two oil drops. Distances to the left of the point of current injection are denoted by $\hat{X}$ and distances to the right by X.

Assuming that the effect of the oil drop was to increase the axial resistance of the axon from a value R_a to a new value R_a', a calculation was done to find the value of R_a' which could account for the observations. In practice the oil drop forms a cylindrical plug probably leaving a thin annulus of axoplasm which provided a small conductive pathway, resulting in the new apparent value for R_a'. A one-dimensional cable model with two semi-infinite compartments separated by an oil drop 500 μm in length was used for the calculation (Fig. 2 C). Using steady-state equations (Taylor, 1963) together with conditions of potential and current continuity at interfaces, the deviation, V, of the transmembrane potential from its resting value was computed in compartment 3 (Fig. 2 C). For a current I injected into compartment 1, value of V for compartment 3 was derived as:

$$V = \frac{-2IR_a \lambda \alpha \beta k e^{(b-x)/\lambda}}{\psi},$$

where $\psi = \alpha^2[(1-k)^2 - (1+k)^2\beta^2]$, $\alpha = e^{a/\lambda}$, $\beta = e^{(b-a)/\lambda'}$, $\lambda = (R_m/R_a)^{1/2}$, $\lambda' = (R_m/R_a')^{1/2}$, and $k = (R_a'/R_a)^{1/2}$. R_m is the membrane resistance per unit area for the given axon. The specific value of the axial resistance chosen was 30 $\Omega \cdot$cm and

specific membrane resistance 1,000 Ωcm². An axon radius of 150 μm was used with $a = 500$ μm and $b = 1{,}000$ μm. In order to account for the experimental results, it was necessary to increase R_a' to 60 times R_a. This indicates an effective oil drop seal, although a very small leakage does occur.

Using the above value for R_a' the potential distribution due to an intracompartmental injection of a current I for a compartment 2,200 μm long bounded by two 500-μm long oil drops was calculated (Fig. 2 D). The formula derived in this case, from steady-state cable theory, was:

$$V = Ae^{x/\lambda} + Be^{-x/\lambda},$$

where $A = -IR_a\lambda\phi(\hat{\phi} - \hat{\psi})/2(\phi\phi - \hat{\psi}\psi)$, $B = IR_a\lambda\psi(\hat{\phi} - \hat{\psi})/2(\phi\phi - \hat{\psi}\psi)$, and $\phi = (1 - k^2)(1 - \beta^2)$. $\hat{\psi}$ and $\hat{\phi}$ are obtained from ψ and ϕ by substituting $\hat{a}$ and $\hat{b}$ for a and b; $\hat{a}$ and $\hat{b}$ refer to distances to the left of the current injection point. Values and parameters were as described above with $a = 2{,}000$ μm, $b = 2{,}500$ μm, $\hat{a} = 200$ μm, $\hat{b} = 700$ μm. Calculations were also made for the case where current was injected into an axon without oil drops. It was found that when 2.5 μA of current was injected 200 μm from one oil drop, the potential at the injecting electrode was 71.5 mV and the potential 2,000 μm away dropped to 87% of this value. However, when the oil drops were absent, the potential at the current injecting electrode was 26.5 mV and 2,000 μm away it had dropped to 67% of the value. The percentage fall-off with distance is illustrated in Fig. 2 B. It is thus clear that oil drops significantly enhance the degree of isopotentiality of the axonal postsynaptic region.

Injection of Tetraethylammonium

After the double oil seal, tetraethylammonium chloride (TEA) was iontophoretically injected from a pipette containing 1 M TEA (pulses of 5×10^{-8} A, 100-ms duration at 2/s). The injection was continued for a period of 2–3 h until delayed rectification was blocked (Armstrong and Binstock, 1965). The electrode was then utilized to inject current pulses while a second electrode was used to record postsynaptic responses. Tetrodotoxin (TTX) was applied after the oil and TEA injections. A special technique developed by Manalis (1971) was utilized; i.e. the bathing solution was lowered below the level of the ganglion and a TTX solution 2×10^{-6} g/ml was applied locally onto the postsynaptic axon with a fine cotton swab. Given the rather restricted portion of the axon isolated by the double intracellular oil gap, the local application of TTX was successful in blocking the action potential postsynaptically. Although some reduction of the presynaptic spike was also observed, its attenuation was not large enough to block synaptic transmission. Since it is known that TTX does not interfere with synaptic transmitter release (Bloedel et al., 1966; Katz and Miledi, 1967; Kusano et al., 1967), this method proved very useful for our purposes.

Current and Voltage Clamp

Current was applied across the membrane of the postsynaptic compartment through a microelectrode filled with 2 M potassium citrate. This current was supplied by an isolation unit with a high series resistance and measured by differential recording

across a 100-Ω resistor. The membrane voltage clamp condition was attained by means of a feedback circuit which allowed the change in membrane potential value to be reintroduced into the current injection circuit as shown in Fig. 1 (Cole, 1949; Hodgkin and Huxley, 1952 *a*). The experiments were controlled and the data processed by a digital computer (PDP 8/E, Digital Equipment Corp., Maynard, Mass.), which sent control potential steps to the voltage clamp circuit via a digital-to-analog converter (DAC 12Q, Analog Devices, Inc., Norwood, Mass.). The current was measured by a currentometric operational amplifier which was sampled at 25-μs intervals by the computer via an analog-to-digital converter (ADC 12Q) (Joyner and Moore, 1973). Due to the low input resistance of the postsynaptic region as compared to the microelectrode resistance, a high voltage (±100 V) control amplifier was used.

RESULTS

Reversal Potential of the EPSP after TEA Injection

In order to demonstrate the reversal of the postjunctional potential, we used the technique originally introduced by Fatt and Katz in 1951. In this method, the end-plate potential (EPP) and a direct action potential in the muscle fiber are superimposed. The action potential observed at the subsynaptic region shows a decrease in peak amplitude and a biphasic decay phase when compared with the spike generated at a nonjunctional level. This is due to the fact that the peak of the action potential is large enough to reverse the direction of the EPP current. The application of a similar method in our isolated segment demonstrated after TEA injection that the EPSP was not reversed at small positive values of the membrane potential.

As shown in Fig. 3, after TEA injection the postsynaptic spike potential was increased in duration and its plateau amplitude was maintained at a positive membrane potential. This prolonged action potential could be generated either by synaptic activation (Fig. 3 B), or by direct activation through current applied through the second intracellular electrode (Fig. 3 C).

Interaction experiments where the EPSP was evoked at different intervals after the postsynaptic spike was generated are shown in Fig. 3 D–F. As illustrated in this figure, the EPSP remained positive although the membrane potential was also positive. As the interval between the onset of the action potential and the EPSP became smaller, the synaptic potential was evoked at a higher level on the falling phase of the spike. Even at membrane potential levels of +15–18 mV the EPSP remained positive.

Reversal of EPSP

CURRENT CLAMP The above type of experiment clearly indicated that in a situation close to isopotential, the reversal of the EPSP still occurred at a positive potential. In order to obtain a membrane with a nearly linear

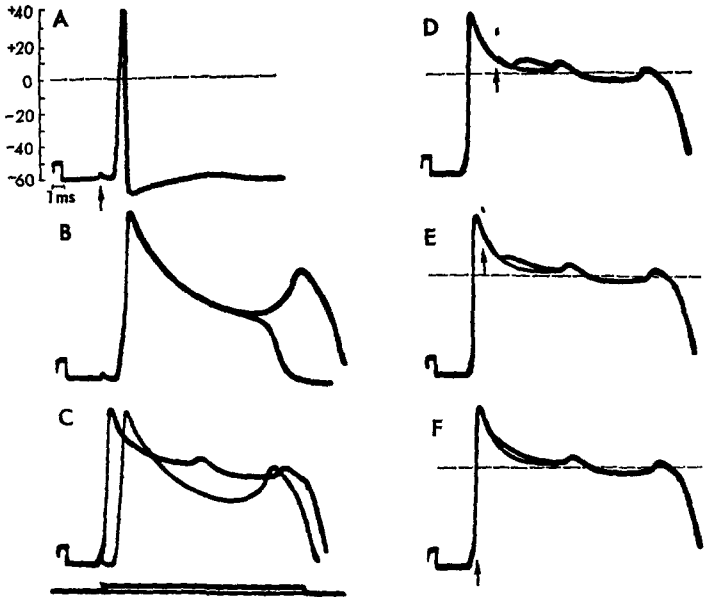

FIGURE 3. Interaction between action potential and synaptic potential after TEA injection in the postsynaptic axon. (A) Synaptically evoked action potential in the postsynaptic fiber. (B) Synaptically evoked action potential in the same fiber after 2 h of TEA injection. (C) Comparison between synaptically evoked action potential and an action potential produced in the same fiber by injection of a prolonged current pulse. (D–F) Action potentials are evoked by current pulse while the presynaptic stimulation is delivered at different intervals (arrow) with respect to onset of the stimulating current. Note in D–F that the EPSP is still positive at positive potential levels. Time and voltage calibration as indicated in figure.

current voltage relationship, TTX was painted onto the postsynaptic fiber (Methods) after TEA injection and double intracellular oil gap. The result of one such experiment is shown in Fig. 4 A. As illustrated in that figure, the reversal occurred at approximately +20 mV, the amplitude of the synaptic potential being rather linear to the membrane potential value. The nonlinearity seen at the beginning of the potential record represents residual G_{Na} since local TTX application does not cover the postsynaptic surface in its entirety.

A similar set of records was obtained in six other preparations, as shown in the plot in Fig. 4 B. As in the case illustrated in Fig. 4 A, these experiments yielded an approximately linear relationship between current and voltage. The range of reversals in this set of results was from +18 to +25 mV with a very small scatter. Since in all of these cases a good double internal gap was obtained, it is concluded that the reversal potential for the EPSP is positive with respect to zero membrane potential.

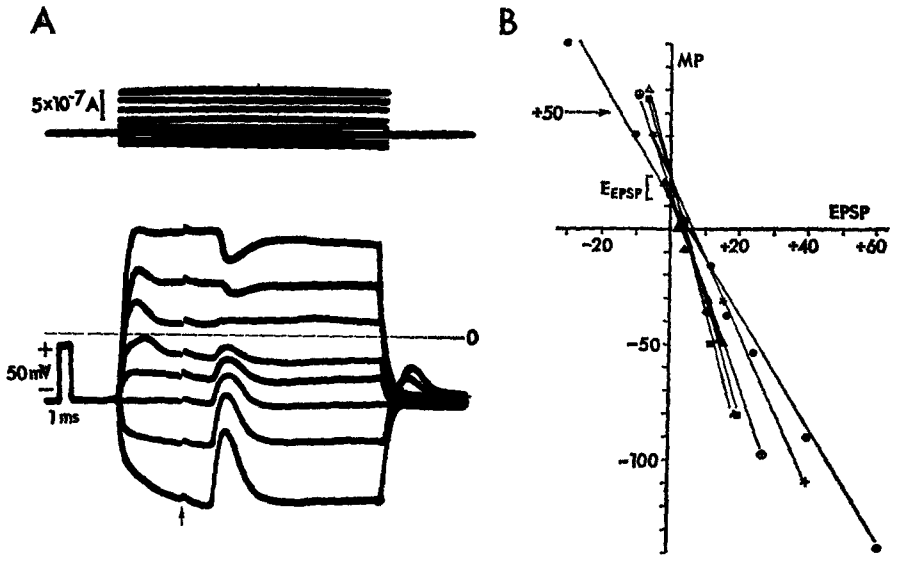

FIGURE 4. Reversal of the EPSP after application of TTX and TEA. (A) Amplitude of the EPSP is seen to increase with hyperpolarizing pulses and to decrease and reverse with depolarizing pulses, the amplitudes of which are indicated in the upper left corner. (B) Plot of the synaptic potential amplitude against membrane potential level. Reversal potentials in these five examples occurred between the levels of 15 and 25 mV positive.

An important question to be settled in these experiments, however, is whether the E_{EPSP} is at E_{Na}. The measurements described above argued against this since E_{Na} is generally >40 mV. However, given the multiple penetration and the time required for the establishment of the experimental paradigm, it was possible that a change in $[Na^+]_i$ could have affected E_{Na} (Moore and Adelman, 1961). To resolve this question, a set of voltage clamp experiments was done and E_{Na} directly compared with E_{EPSP}.

VOLTAGE CLAMP The voltage clamp technique was used to determine the time-course and reversal potential of the synaptic current as well as the value of E_{Na}. The membrane potential was held at a constant hyperpolarizing level (—100 mV), and at 10-s intervals the potential was driven for 12 ms to some pulse potential between −150 and +100 mV in 10-mV steps. The stimulus to the presynaptic axon was set to occur at a time such that the synaptic conductance change occurred after the active K^+ conductance had reached a steady value.

Thus, for depolarizing potential steps, the current record consists of the capacitive, the active Na^+, the active K^+, and the postsynaptic currents (Fig. 5 A). Since the current resulting from a hyperpolarizing potential step consists of a capacitive current and a steady leakage current (Hodgkin and Huxley; 1952 *a*), this current was used to "leak-correct" the current records

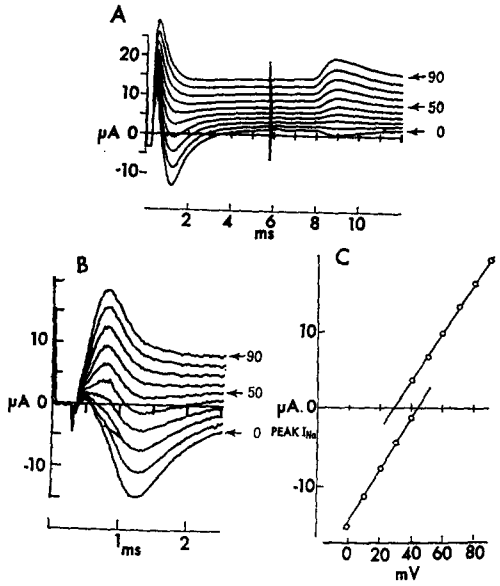

FIGURE 5. Experimental measurement of E_{EPSP} and E_{Na}. (A) Experimentally measured currents corresponding to a family of step clamps from −100 mV to the potentials indicated for each curve. The artifact from the presynaptic nerve stimulation recurs about 6 ms from clamp onset and synaptic currents begin at about 8 ms. (B) Leak-corrected experimentally measured currents for a family of step clamps from −100 mV to the potential indicated for each curve. (C) Plot of early peak current (Na^+ current) versus the control potential for the data shown in B.

resulting from a depolarizing potential step. The first 1–2 ms of the leak-corrected currents are mainly Na^+ current since the active K^+ currents were reduced by the use of internal TEA and their time-course is slower than the active Na currents. Fig. 5 B shows the leak-corrected currents from the records of Fig. 5 A.

The active Na^+ currents clearly reverse in sign as the membrane potential is pulsed from −100 mV to 0, +10, +20 . . . +90 mV. At intermediate voltage levels, the currents are biphasic due to the inability of the voltage clamp circuit to make the membrane potential instantaneously follow the command potential. If the maximum Na^+ current at each voltage level is plotted against the membrane potential (Fig. 5 C), there is a discontinuity in the current-voltage relationship at the transition from negative to positive Na^+ currents. This discrepancy is present because the voltage step is not instantaneous. As shown below, the intercept of the current-voltage relationship for the negative currents gives the more accurate determination of E_{Na}. In five experiments the difference in the voltage intercept for the positive and negative currents varied from 0 to 15 mV.

In order to check the validity of the voltage clamp results, the Hodgkin and Huxley

equations (1952 *b*) were utilized to obtain values for Na currents resulting from a perfect voltage clamp (Joyner, 1973) and compare them with the currents that would be obtained using the experimentally measured voltages in our research. The equations were formulated for a temperature of 6.3°C and a Q_{10} of 2 was utilized (Guttman, 1968).

Due to the many problems involved in passing current through a microelectrode, the membrane potential in our experiments did not follow the command potential exactly. At potentials lower than E_{Na}, the potential transiently rose above the command potentials as the membrane potential was driven toward E_{Na} by the increase in the Na^+ conductance. At potentials above E_{Na}, the same driving force caused the membrane potential to rise more slowly to the command potential.

Fig. 6 B shows the Na^+ current computed for a perfect voltage clamp for command

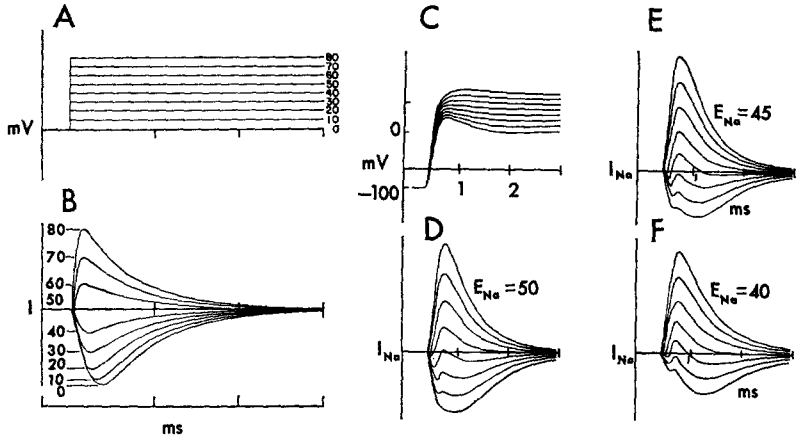

FIGURE 6. Na^+ currents computed from the Hodgkin-Huxley equation. (A–B) Voltage and Na^+ currents computed for perfect voltage control. (C–F) Experimentally measured voltage and corresponding computed Na^+ currents with E_{Na} set to +50 (D), +45 (E), and +40 mV (F). In each case the holding potential is −100 mV and the control potential is 0, 10, 20 . . . 80 mV.

potentials of 0, 10, 20 . . . 80 mV and a holding potential of −100 mV. The Na^+ currents reverse in sign at E_{Na} (+50 mV) and show a decrease in the time to peak with increasing potential. The currents are not biphasic at any potential. The computations of Fig. 6 D–F were obtained using the measured membrane potential, which is shown in Fig. 6 C as the voltage function for the Hodgkin-Huxley equations. This potential was sampled at 25-μs intervals during the experiment and then at a later time successive measured values were used for successive time intervals of the integration of the equations. This was done for theoretical values of E_{Na} = +50, 45, and 40 mV and the corresponding Na^+ currents are shown in Fig. 6 D–F.

Comparison of the simulated currents of Fig. 6 E to the leak-corrected measured currents of Fig. 5 B shows that the data can be reproduced quite well with a Hodgkin-Huxley equation solution using the measured membrane potential from the experiment, there being, as in the experimental case, a discrepancy between the extrapolated

voltage intercept of the negative and positive peak currents. In particular, the computed Na currents for command potentials near E_{Na} show a biphasic course and the time to peak shows the same relationship with the command potential as the experimental data. Note that, in Fig. 6 D–F, if E_{Na} is set equal to +40 or +50 mV, there is far less agreement with the leak-corrected measured currents of Fig. 5 B. The intercept of the plot of the maximum negative Na currents of Fig. 5 B against potential (+44 mV) agrees very well with the result of +45 mV from the simulations just described, while the intercept for the maximum positive Na currents (+29 mV) is considerably lower. Since the time to peak for the negative Na current is greater than the time to peak of the positive Na currents, the determination of E_{Na} would be expected to be more accurate than the voltage intercept of the negative Na currents since the membrane potential is closer to the command potential at the later time. This analysis indicates that the determination of E_{Na} from the intercepts of the plot of the negative peaks versus potential is probably accurate to within 5 mV of the true E_{Na}.

The postsynaptic currents (PSC) were isolated from the data of Fig. 5 by selection of a point in time just before the onset of synaptic transmission and then plotting the deviation from the value at this point for each record for the following 3 ms (Fig. 7 A). The synaptic currents also reverse in sign as the membrane potential is pulsed to successively higher levels, and Fig. 7 B is a plot of PSC versus membrane potential showing a reversal potential of +15 mV.

The data from the five experiments is summarized in Table I. If it is assumed that the synaptic conductance is a combination of Na^+ and K^+ conductance in some fixed ratio, then it is clear that decreases in E_{Na} which

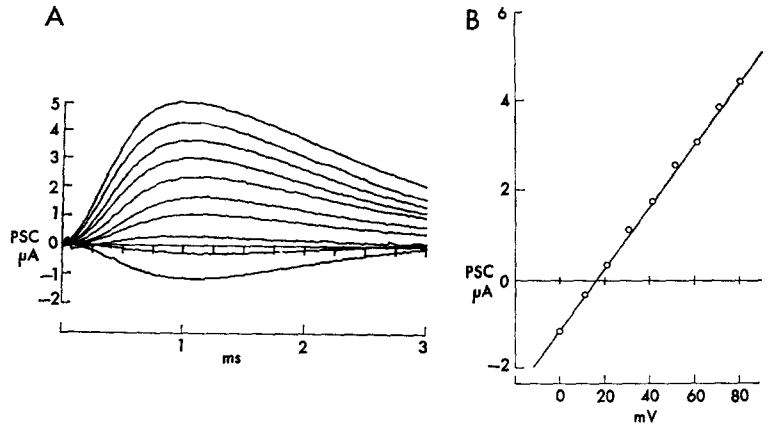

FIGURE 7. Time-course and reversal of synaptic currents. (A) Plot of postsynaptic current (PSC) versus time for a family of step clamps from −100 mV to 0, 10 . . . 90 mV. (B) Plot of postsynaptic current (PSC) versus the control potential for a family of step clamps from −100 mV to 0, 10 . . . 90 mV.

TABLE I

MEASUREMENT OF EPSP REVERSAL POTENTIALS

Exp no.	E_{Na}	E_{EPSP}	g_{Na}	g_s	$g_s(Na^+)/g_s(K^+)$	E^*_{EPSP}
	mV	*mV*	*mmho*	*mmho*		*mV*
1	44	15	0.32	0.07	3.3	19.6
2	42	20	0.19	0.023	4.5	26.6
3	49	24	0.16	0.03	4.2	24.8
4	41	23	0.27	0.014	5.7	30.5
5	32	15	0.34	0.01	5.6	30.5
Mean±SD	42±6	19±4	0.26±.07	0.03±.024	4.6±1.0	26.4±4.5

occur over time will lower the measured value of E_{EPSP}, if E_K is assumed to be constant at −80 mV. However, if E_{Na} is determined experimentally, we can use this measured E_{Na} to correct the measured E_{EPSP} to the value of E_{EPSP} at $E_{Na} = +50$ mV, which we will call E^*_{EPSP}. If $g_s(Na^+)$ and $g_s(K^+)$ are the Na^+ and K^+ components of synaptic conductance then, using the measured values for E_{Na} and E_{EPSP}, we can compute:

$$X = \frac{g_s(K^+)}{g_s(Na^+) + g_s(K^+)} = \frac{E_{Na} - E_{EPSP}}{E_{Na} - E_K}.$$

Then, using this ratio, we can compute:

$$E^*_{EPSP} = 50 - 130\,X.$$

Table I shows the measured values for E_{Na} and E_{EPSP} as well as the corrected values for E_{EPSP} (E^*_{EPSP}).

Time-Course of Synaptic Current at Different Levels of Membrane Potential

At the neuromuscular junction, it was noted by Takeuchi and Takeuchi (1959) that the synaptic current (end-plate current or EPC) had a longer time-course when the membrane potential was held at a hyperpolarizing level. They suggested that the hyperpolarizing current might be preventing the release of acetylcholine from the postsynaptic membrane. Gage and Armstrong (1968) voltage clamped the neuromuscular junction at membrane potentials equal to E_K and E_{Na} using TTX to block action potentials and, from the large difference in the time constant of decay for the miniature EPC's at the two voltage levels, suggested that the transmitter opened separate channels for Na^+ and K^+ with different time-courses.

Kordas (1969) treated muscles with glycerol to block contraction of the muscle fiber over a wide range of voltage clamp potentials and showed a

continuous decrease in the time constant for decay of the EPC as the membrane was held at more depolarizing membrane potentials. If two channels were opened with different time-course, there would be some potentials at which the EPC would be diphasic; however, no diphasic EPC's were seen. Kordas suggested that acetylcholine caused an increase in the Na^+ and K^+ conductance via a single channel which had a voltage-sensitive time-course. This voltage sensitivity of the EPC has been studied extensively by Magleby and Stevens (1972) and the proposed voltage dependence has been used to formulate a theory of the action of acetylcholine that involves the dipole moment of the acetylcholine-receptor complex. The magnitude of the change in time constant for decay of the EPC is from 1.6 ms at a potential of -100 mV to 0.4 ms at a potential of $+90$ mV.

The time-course of the PSC at the squid giant synapse was studied to determine if the membrane potential changed the rate of decline of the falling phase. For several levels of membrane potential in each experiment, the PSC's were isolated from the data records as in Fig. 5 and then each PSC was converted to a function between 0 and 1 by scaling each point in the PSC by the maximum value of the PSC. The natural logarithm of this function for PSC's at membrane potentials of -100 mV and $+90$ mV are shown in Fig. 8. The curve for $V = +90$ mV has more noise than the one for $V = -100$ mV, but it is clear that the time-courses are essentially identical. A total of 3 ms from the start of the PSC was plotted in each case and the time constant was determined as the negative reciprocal of the slope of the linear decreasing phase on the logarithmic scale.

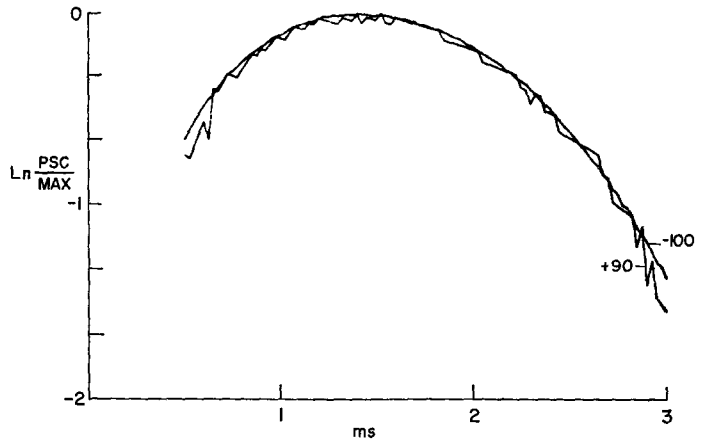

FIGURE 8. Comparison of time-course for synaptic current at two different membrane potential levels. Two curves show a lack of change in the time-course for synaptic potential evoked at -100- and $+90$-mV membrane potential. For further explanation, see text.

The average values (five experiments) for the time constant of decay of the PSC at −100 mV and at +90 mV was 0.85 + 0.21 ms and 0.94 ± 0.18 ms, respectively (mean ± SD). Even this small difference is probably explained by the slow rise in the K^+ conductance which had persisted until the time of the synaptic conductance change. This slowly rising base line would increase the apparent decay time constant at depolarizing levels. It must be concluded therefore that, as opposed to the findings in the neuromuscular junction, the time-course of the synaptic current in the squid giant synapse does not appear to be substantially modified by the potential across the postsynaptic-subsynaptic membrane.

Effect of Synaptic Collaterals on Reversal Potential

Recently, Young (1973) has shown that the postsynaptic axon establishes synaptic contact with the presynaptic axon by means of numerous narrow branching collaterals. Since the main body of the postsynaptic axon is separated from the synaptic site by the collaterals, the measured reversal potential may be overestimated. However, electron microscopical studies by D. E. Hillman (personal communication) have established that the actual synaptic contacts may occur at different distances along these branchlets (i.e., the synapse is actually distributed along these small cables rather than restricted to their terminal portion).

It seems likely that anatomical variations in the collateral dimensions at different synapses would introduce variability in the determination of the measured reversal potential which would not be reduced by increasing the isopotentiality of the main postsynaptic region. However, the consistent results obtained with the oil gap method led us to believe that the effects of the collaterals are small, especially given the distributed nature of the synaptic contact along the postsynaptic axon collaterals. Furthermore, the synapses situated near the base of the collaterals would see the same potential as the giant axon and would be the most prominent in generating the initial part of the EPSP, and the first to reverse. Since no obvious biphasicity was observed at the reversal level, it must be assumed that under the present oil gap conditions the synapse cannot be regarded as a strongly distributed synapse.

DISCUSSION

Among the most important questions to be resolved at this juncture regarding the generation of synaptic potentials is the nature of the ionic conductance changes. Indeed, the types of conductances necessary for the generation of an EPSP with a reversal potential of −15 mV are quite different from those described in our results. In fact, rather than a close to 1:1 ratio between Na^+ and K^+, a ratio of close to 4.6:1 may be operant. Unfortunately, attempts

to determine this ratio directly by varying $[K^+]_o$ gave equivocal results. The functional integrity of the synaptic junction was easily disrupted by varying $[K^+]_o$ in a sufficient range to allow a quantitative measurement without drastically changing the properties of the synaptic membrane.

The large variability in the published determinations of reversal potential at the squid giant synapse is most likely produced by two main factors. The first is the decrease in E_{Na} which accompanies membrane damage from any source and which also occurs gradually over time (Moore and Adelman, 1961). Since the value of E_{Na} is needed to compute the ratio of synaptic Na^+ conductance to synaptic K^+ conductance, the ability to reverse the active Na^+ currents with the oil drop technique to give a determination of E_{Na} simultaneously with and independently of the determination of the normal E_{EPSP} is essential for the computation. Decreases of E_{Na} cause decreases in E_{EPSP}, and these could not be detected or corrected if E_{Na} were not measured. The corrections we have applied are based on the assumption of an accurately estimated E_{Na} (± 5 mV), a stable E_K, and participation of only Na^+ and K^+ ions in the synaptic conductance change.

The second factor contributing to the variability of the published results is the spatial spread of the synaptic region and, therefore, the nonisopotentiality of the postsynaptic region when current is injected at a point within that region (Miledi, 1969; Manalis, 1971). The feasibility and limitations of a microelectrode voltage clamp of nonisopotential regions has been studied with computer simulations of an active cable in the feedback loop of a voltage clamp circuit (Joyner et al., in preparation). The different voltage profiles within the synaptic region set up by different placements of the current and voltage electrodes lead to errors in the determination of E_{EPSP} which can be positive or negative depending on the relative positions of the electrodes. These errors are increased in magnitude as the specific resistance of the membrane is lowered and, therefore, are particularly large if TEA is not used to limit the K^+ conductance. It must be kept in mind, however, that TEA may have an effect on either the time dependence, voltage dependence, or ionic selectivity of the postsynaptic receptor, or could carry outward synaptic current.

The point of consequence here is whether the ratio of Na^+ to K^+ permeability for a given patch of subsynaptic-postsynaptic membrane is a set value, or whether the ratio can change either in a given postsynaptic area or for given synapses. An important consideration regarding these findings is whether the difference in the Na^+ to K^+ ratio observed here, in contrast to the neuromuscular junction, is (*a*) the product of a different ratio for Na and K "channels" which may vary independently of each other or (*b*) whether that ratio of Na^+ to K^+ permeability can vary given a single class of "channel." Clearly the present experiments cannot resolve this issue; however, they

do raise the possibility that the ionic permeability ratio between Na^+ and K^+ may be different for different synapses. Should this type of variation be found in other synapses, the implications of these findings would be of great interest, especially in the central nervous system. Here the possibility of varying the ionic mechanism from predominantly Na^+ to predominantly K^+ would result in the possibility of regulating synaptic efficacy at a molecular level. Thus, besides the integrative properties inherent in the geometry of nerve cells, a second parameter which could at least hypothetically change would be the Na^+ to K^+ permeability ratio at individual subsynaptic patches.

The authors are indebted to Drs. J. W. Moore and F. Ramon for their constructive discussion on the voltage clamp results and to Dr. Moore for space and computer equipment for the voltage clamp experiments.

This study was supported by U.S.P.H.S. research grants NS-09916 and NS-03437 from the National Institute of Neurological Diseases and Stroke.

Received for publication 20 February 1974.

REFERENCES

ARMSTRONG, C. M., and L. BINSTOCK. 1965. Anomalous rectification in the squid giant axon injected with tetraethylammonium chloride. *J. Gen. Physiol.* **48**:859.

BAKER, P. F., A. L. HODGKIN, and T. I. SHAW. 1962. The effects of charges in internal ionic concentrations on the electrical properties of perfused giant axons. *J. Physiol. (Lond.).* **164**:355.

BLOEDEL, J. R., P. W. GAGE, R. LLINÁS, and D. M. J. QUASTEL. 1966. Transmitter release at the squid giant synapse in the presence of tetrodotoxin. *Nature (Lond.).* **112**:49.

COLE, K. S. 1949. Dynamic electrical characteristics of the squid axon membrane. *Arch. Sci. Physiol.* **3**:253.

FATT, P., and B. KATZ. 1951. An analysis of end-plate potentials recorded with intracellular electrodes. *J. Physiol. (Lond.).* **115**:320.

GAGE, P. W., and C. M. ARMSTRONG. 1968. Miniature end-plate currents in voltage clamped muscle fibers. *Nature (Lond.).* **218**:363.

GAGE, P. W., and J. W. MOORE. 1969. Synaptic currents at the squid giant synapse. *Science (Wash. D. C.).* **166**:510.

GUTTMAN, R. 1968. Temperature dependence of accommodation and excitation in space clamped axons. *J. Gen. Physiol.* **51**:759.

HODGKIN, A. L., and A. F. HUXLEY. 1952 *a*. Currents carried by sodium and potassium ions through the membrane of the giant axon of *Loligo*. *J. Physiol. (Lond.).* **116**:449.

HODGKIN, A. L., and A. F. HUXLEY. 1952 *b*. A quantitative description of membrane current and its application to conduction and excitation in nerve. *J. Physiol. (Lond.).* **117**:500.

JOYNER, R. W. 1973. Measurement and analysis of ionic currents at the squid giant synapse. Ph.D. Thesis, Duke University, Durham, N. C.

JOYNER, R. W., and J. W. MOORE. 1973. Computer controlled voltage clamp experiments. *Ann. Biomed. Eng.* **1**:368.

KATZ, B. and R. MILEDI. 1967. A study of synaptic transmission in the absence of nerve impulses. *J. Physiol. (Lond.).* **192**:407.

KORDAS, M. 1969. The effect of membrane polarization on the time course of the EPC in frog sartorius muscle. *J. Physiol. (Lond.).* **204**:493.

KUSANO, K., D. R. LIVENGOOD, and R. WERMAN. 1967. Correlation of transmitter release with membrane properties of the presynaptic fiber of the squid giant synapse. *J. Gen. Physiol.* **50**:2579.

LLINÁS, R., and C. NICHOLSON. 1972. Reversal potential for EPSP in squid stellate ganglion tested in isopotential conditions. *Biophys. Soc. Annu. Meet. Abstr.* **12**:70*a*.

MAGLEBY, K. L., and C. F. STEVENS. 1972. The effect of voltage on the time course of end-plate current. *J. Physiol. (Lond.)*. **223**:151.

MANALIS, R. S. 1971. PSP reversal potential measurements in the squid giant synapse. *Biophys. Soc. Annu. Meet. Abstr.* **12**:130*a*.

MILEDI, R. 1969. Transmitter action in the giant synapse of the squid. *Nature (Lond.)*. **223**:1284.

MILEDI, R., and C. R. SLATER. 1966. The action of calcium on neuronal synapses in the squid. *J. Physiol. (Lond.)*. **184**:473.

MOORE, J. W., and W. J. ADELMAN. 1961. Electronic measurement of the intracellular concentration and net flux of sodium in the squid axon. *J. Gen. Physiol.* **45**:77.

TAKEUCHI, A., and N. TAKEUCHI. 1959. Active phase of frog's end-plate potential. *J. Neurophysiol.* **22**:395.

TAKEUCHI, A., and N. TAKEUCHI. 1962. Electrical changes in pre- and post-synaptic axons of the giant synapse of *Loligo*. *J. Gen. Physiol.* **45**:1181.

TAYLOR, R. E. 1963. Cable theory. *In* Physical Techniques in Biological Research, Vol. VI, Electrophysiological Methods, Part B. W. L. Nastuk, editor. Academic Press, Inc., New York.

WERMAN, R. 1972. CNS cellular level: Membranes. *Ann. Rev. Physiol.* **34**:337.

YOUNG, J. Z. 1973. The giant fibre synapse of *Loligo*. *Brain Res.* **57**:457.